Tsai et al.:

Risk-Based Prioritization of PFAS using Phenotypic and Transcriptomic Data from Human Induced Pluripotent Stem Cell-Derived Hepatocytes and Cardiomyocytes

Supplementary Data

List of supplementary files

- **Supplementary File 1:** Phenotypic raw data of induced pluripotent stem cell-derived hepatocytes, provided seperately as SuppFile1_iPSCHep_Phenotypic_Raw.csv. doi:10.14573/altex.2311031s1
- **Supplementary File 2:** Phenotypic raw data of induced pluripotent stem cell-derived cardiomyocytes, provided seperately as SuppFile2_iPSCCM_Phenotypic_Raw.csv. doi:10.14573/altex.2311031s2
- **Supplementary File 3:** BMDExpress output of induced pluripotent stem cell-derived hepatocytes, provided seperately as SuppFile3_BMD_iPSCHep.txt. The BMD values were calculated based on concentrations at 0 (DMSO controls), 0.1 µM, 1 µM, and 10 µM. doi:10.14573/altex.2311031s3
- **Supplementary File 4:** BMDExpress output of induced pluripotent stem cell-derived endothelial cells, provided seperately as SuppFile4_BMD_ iPSCCM.txt. The BMD values were calculated based on concentrations at 0 (DMSO controls), 0.1 µM, 1 µM, and 10 µM. doi:10.14573/altex.2311031s4
- **Supplemental File 5:** List of significant combinations of gene/categorical comparison using post hoc Tukey's Tests conducted to compare categorical differences in log-2-fold-change values between individual PFAS treatments (10 µM samples) and control samples. These tests were applied to genes that demonstrated significance in the ANOVA analysis, with adjusted p-values set at the 0.05 level. doi:10.14573/altex.2311031s5
- **Supplemental File 6:** List of significantly enriched pathways, the corresponding higher-level nodes based on the REACTOME pathway hierarchy, and the -$\log_{10}$-transformed q-value for each enriched pathway in iPSC-Hep, provided seperately as SuppFile5_pathways_ iPSCHep.csv. NA indicates not significant. doi:10.14573/altex.2311031s6
- **Supplemental File 7:** List of significantly enriched pathways, the corresponding higher-level nodes based on the REACTOME pathway hierarchy, and the -$\log_{10}$-transformed q-value for each enriched pathway in iPSC-CM, provided seperately as SuppFile6_pathways_ iPSCCM.csv. NA indicates not significant. doi:10.14573/altex.2311031s7

doi:10.14573/altex.2311031s8

Tab. S1: List of human steady-state plasma concentrations (in µM) and exposure values for 18 PFAS that had available data from either source

Chemical_Name	Abbr	Css (µM)	Css_Data_Source	95th_Exposure_value
4:2 Fluorotelomer alcohol	4:2 FTOH	19.48	Kreutz_2023	4.79E-05
Perfluorobutanesulfonic acid	PFBS	78.99	httk R package	0.005383
8:2 Fluorotelomer sulfonic acid	8:2 FTS	1437	Smeltz_2023	7.43E-05
6:2 Fluorotelomer sulfonic acid	6:2 FTS	83.63	Smeltz_2023	0.002178
Nonafluoropentanamide	PFNAM	9.549	Kreutz_2023	5.56E-05
Perfluorohexanesulfonamide	PFHxSA	2268	Smeltz_2023	6.19E-05
3:3 Fluorotelomer carboxylic acid	3:3 FTCA	159	Smeltz_2023	7.26E-05
Perfluorooctanoic acid	PFOA	205.3	httk R package	2.34E-05
Perfluorotetradecanoic acid	PFTeDA	491.1	Smeltz_2023	6.47E-05
Ammonium perfluorooctanoate	NH4PFOA	257	httk R package	0.079706
Perfluorodecanoic acid	PFDA	344.4	httk R package	2.62E-05
Perfluoroundecanoic acid	PFUnDA	6878	httk R package	8.06E-06
Perfluorononanoic acid	PFNA	865.9	httk R package	2.40E-05
Perfluoroheptanoic acid	PFHpA	651.8	httk R package	0.000227
Perfluoro-3,6-dioxaoctane-1,8-dioic acid	PFHx2Et2OA	119.5	Smeltz_2023	7.03E-05
Perfluoro-3-methoxypropanoic acid	PFMPA	24.73	Smeltz_2023	9.79E-05
Perfluoro-3,6,9-trioxatridecanoic acid	PFPE-6	527.5	Smeltz_2023	6.83E-05
Perfluoro(4-methoxybutanoic) acid	PFMOBA	104.8	Smeltz_2023	7.79E-05

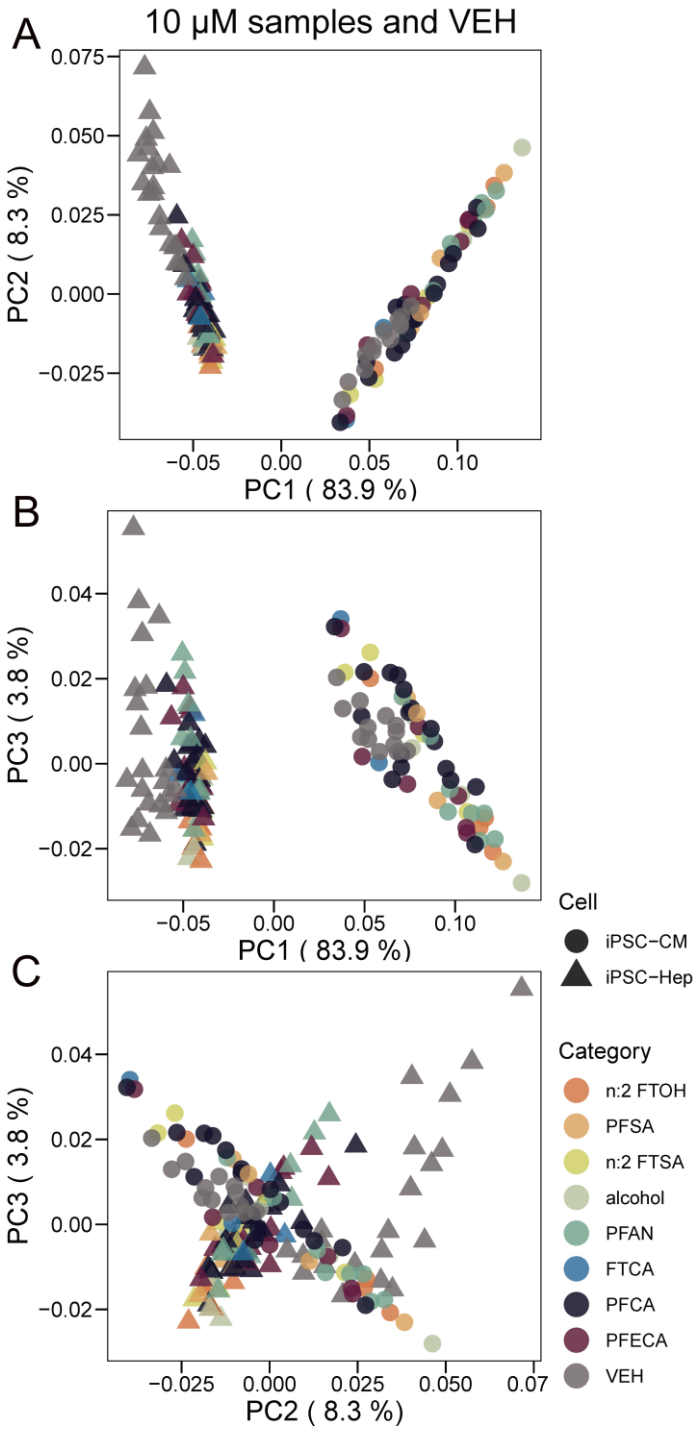

Fig. S1: Principal component analysis (PCA) of gene expression data performed on all samples treated with 10 µM of the tested PFAS in both iPSC-Hep and iPSC-CM
(A) PCA on PC1 and PC2. (B) PCA on PC1 and PC3. (C) PCA on PC2 and PC3. In all panels, each dot represents an individual sample, while the colors correspond to different categories, and shapes correspond to different cell types (as indicated in the inset).

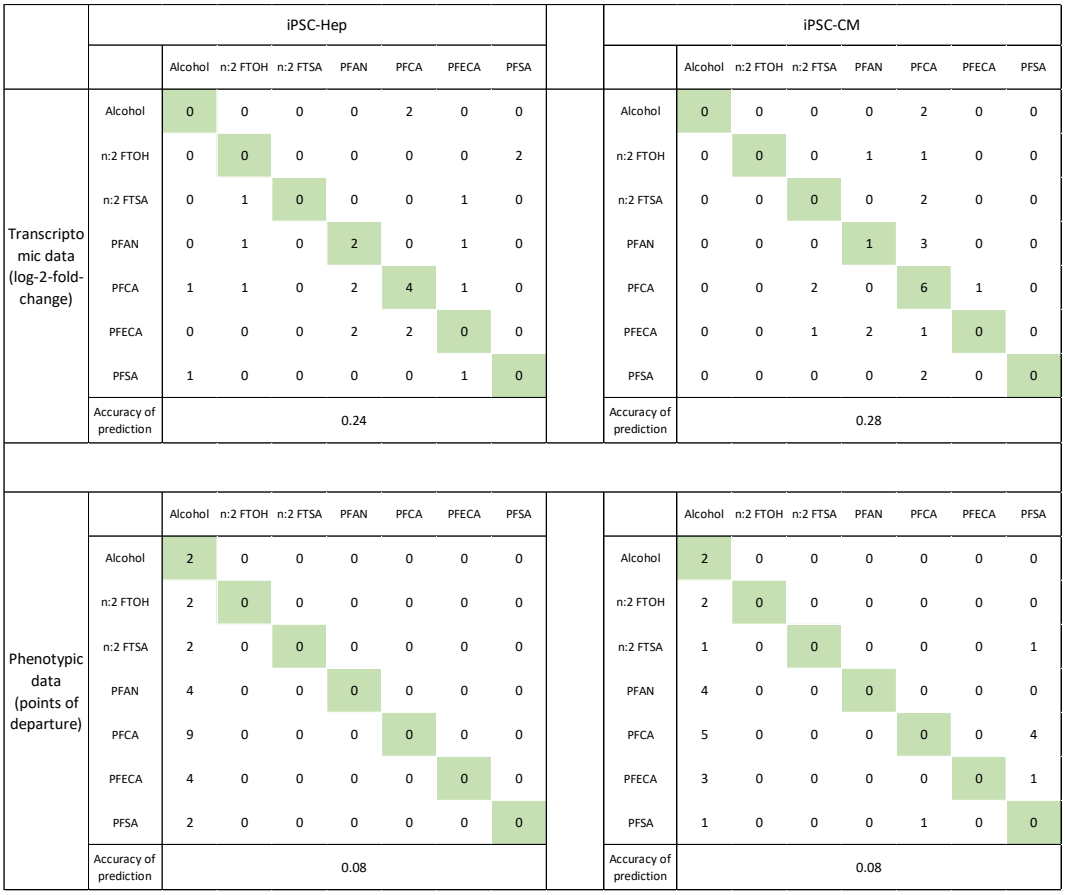

		iPSC-Hep								iPSC-CM							
		Alcohol	n:2 FTOH	n:2 FTSA	PFAN	PFCA	PFECA	PFSA		Alcohol	n:2 FTOH	n:2 FTSA	PFAN	PFCA	PFECA	PFSA
Transcriptomic data (log-2-fold-change)	Alcohol	0	0	0	0	2	0	0		Alcohol	0	0	0	0	2	0	0
	n:2 FTOH	0	0	0	0	0	0	2		n:2 FTOH	0	0	0	1	1	0	0
	n:2 FTSA	0	1	0	0	0	1	0		n:2 FTSA	0	0	0	0	2	0	0
	PFAN	0	1	0	2	0	1	0		PFAN	0	0	0	1	3	0	0
	PFCA	1	1	0	2	4	1	0		PFCA	0	0	2	0	6	1	0
	PFECA	0	0	0	2	2	0	0		PFECA	0	0	1	2	1	0	0
	PFSA	1	0	0	0	0	1	0		PFSA	0	0	0	0	2	0	0
	Accuracy of prediction	0.24								Accuracy of prediction	0.28						

		Alcohol	n:2 FTOH	n:2 FTSA	PFAN	PFCA	PFECA	PFSA		Alcohol	n:2 FTOH	n:2 FTSA	PFAN	PFCA	PFECA	PFSA
Phenotypic data (points of departure)	Alcohol	2	0	0	0	0	0	0		Alcohol	2	0	0	0	0	0	0
	n:2 FTOH	2	0	0	0	0	0	0		n:2 FTOH	2	0	0	0	0	0	0
	n:2 FTSA	2	0	0	0	0	0	0		n:2 FTSA	1	0	0	0	0	0	1
	PFAN	4	0	0	0	0	0	0		PFAN	4	0	0	0	0	0	0
	PFCA	9	0	0	0	0	0	0		PFCA	5	0	0	0	0	0	4
	PFECA	4	0	0	0	0	0	0		PFECA	3	0	0	0	0	0	1
	PFSA	2	0	0	0	0	0	0		PFSA	1	0	0	0	1	0	0
	Accuracy of prediction	0.08								Accuracy of prediction	0.08						

Fig. S2: Analysis of the categorical prediction using gene expression data and phenotypic bioactivity data using the Prediction Analysis of Microarrays classification procedure

Top: The results of supervised analysis in which the PFAS category is predicted from the log-2-fold-change values derived from differential gene expression using highest tested concentration samples versus control samples in iPSC-Hep (top-left) and iPSC-CM (top-right). Bottom: The results of supervised analysis in which the PFAS category is predicted from the phenotypic points of departure in iPSC-Hep (bottom-left) and iPSC-CM (bottom-right). Each row refers to the true category and columns to predicted category. Correct classification counts are colored in green as values on the diagonal. Correct classification rates are shown in last row of each panel.

Combined data: phenotypic points of departure and transcriptomic log-2-fold-change values in both cell types							
	Alcohol	n:2 FTOH	n:2 FTSA	PFAN	PFCA	PFECA	PFSA
Alcohol	1	0	0	0	1	0	0
n:2 FTOH	1	0	1	0	0	0	0
n:2 FTSA	0	0	0	1	0	1	0
PFAN	3	0	0	0	1	0	0
PFCA	7	0	1	0	0	1	0
PFECA	1	1	0	0	2	0	0
PFSA	0	0	0	0	2	0	0
Accuracy of prediction	0.04						

Fig. S3: Analysis of the categorical prediction using combined gene expression data and phenotypic points of departure data using the Prediction Analysis of Microarrays classification procedure
The results of supervised analysis in which the PFAS category is predicted from the log-2-fold-change values derived from differential gene expression using highest tested concentration samples versus control samples, and from all phenotypic points of departure in both iPSC-Hep and iPSC-CM. Each row refers to the true category and columns to predicted category. Correct classification counts are colored in green as values on the diagonal. Correct classification rate is shown in last row.

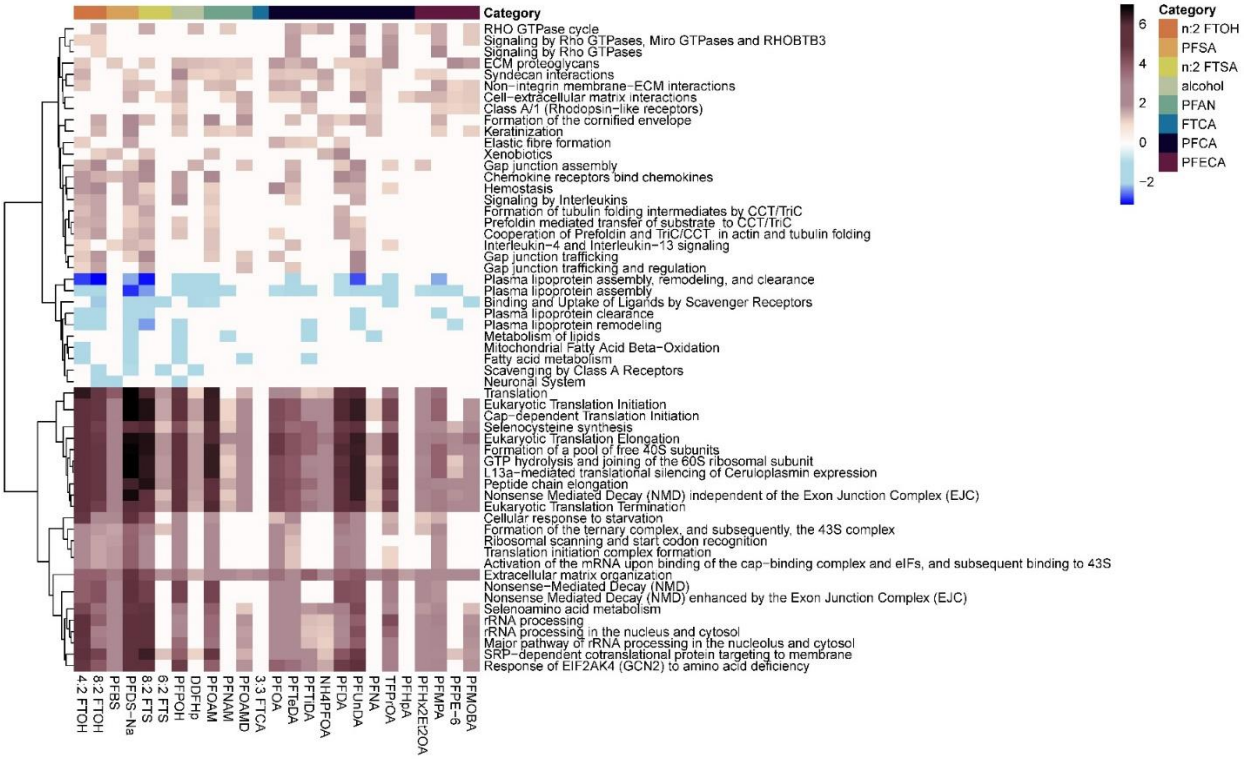

Fig. S4: A heatmap of Reactome pathways significantly enriched in iPSC-Hep
Pathways are color-coded, with brown shades indicating up-regulated pathways and blue shades representing down-regulated pathways. Darker shades indicate lower p-values. The PFAS are ordered based on their respective categories. See Tab. 1 for class and individual chemical abbreviations.

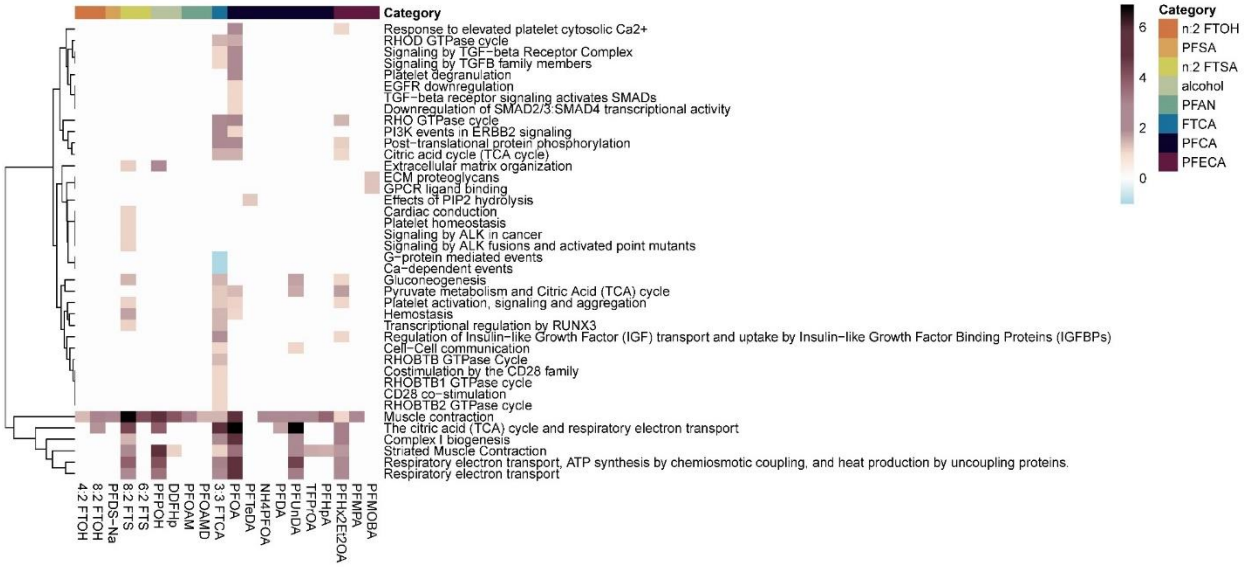

Fig. S5: A heatmap of Reactome pathways significantly enriched in iPSC-CM
Pathways are color-coded, with brown shades indicating up-regulated pathways and blue shades representing down-regulated pathways. Darker shades indicate lower p-values. The PFAS are ordered based on their respective categories. See Tab. 1 for class and individual chemical abbreviations.